https://doi.org/10.46344/JBINO.2022.v11i05.19

IN SILICO ANALYSIS OF QUANTUM-CHEMICAL INTERACTIONS OF INDOLEACETIC ACID VS. AMINO ACIDS

[1,2] **Manuel González-Pérez, [1]Adriana Reyes-Castro, [1]Juventino Reza-Salgado, [1]Jesús Antonio Salazar-Magallón, [1]Pedro Antonio Rodríguez-Salazar, [1]Sergio Gómez-Ramos, [1]Orlando Tlakaelel Notario-Rendón.**

[1]Universidad Tecnológica de Tecamachalco. Ingeniería en Agricultura Sustentable y Protegida.
[2]Tecnológico Nacional de México, campus Tepeaca. Subdirección de investigación.

Email : manuel.gp@tepeaca.tecnm.mx

ABSTRACT

Indole-3-acetic acid (IAA) is a natural phytohormone, a precursor of the active form of auxin. This acid comes from the amino acid L-tryptophan (Trp). Some scientists found that high doses of cisplatin in cancer patients increase urinary and plasma levels of IAA but do not affect platelets or plasma-free serotonin. This research aimed to calculate the quantum-chemical interactions of indoleacetic acid and protein amino acids through computational quantum chemistry in silicon. The characterization of the IAA was carried out through the hyperchem simulator and its manual. All calculations were based on electron transfer coefficient (ETC) theory. We did a chi-square hypothesis association test to determine a nonlinear pattern. We made a box-and-whisker plot to demonstrate this nonlinear pattern. The most robust IAA interactions in terms of electron affinity with AAs are Arg and His. IAA behaves as an oxidizing agent in the first quartile's interactions. The specific pattern exhibited by this anchor is expected with a positive bias. We can predict that IAA does not destroy cancerous tumors.

KEYWORDS
In silico laboratory, quantum-chemical interactions, indoleacetic acid, amino acids, proteins.

INTRODUCCIÓN

Indole-3-acetic acid (IAA) is a natural phytohormone. It is a precursor of the active form of auxin. This acid comes from the amino acid L-tryptophan (Trp). In the transformation of Trp to IAA, the indole group remains constant (Fig. 1).

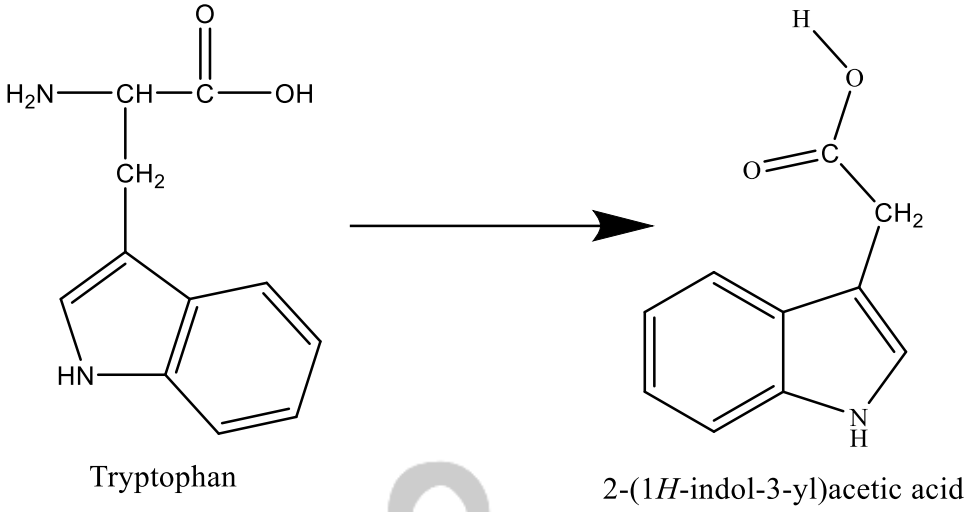

Figure 1. Conversion of tryptophan to IAA. Deamination.

Application of indoleacetic acid.

Gravel and Tweddell (2007), in their investigations, showed that the roots of tomato seedlings grown in the presence of increasing concentrations of IAA (0-10 µg/ml) were significantly longer when the seeds were previously treated with P. putida or T atroviride, on the other hand, Saber et al. (2017) investigated the efficiency of two Trichoderma harzianum isolates (WKY1 and WKY5) as biocontrol agents against anthracnose disease in sorghum. They found that, under greenhouse conditions, the application of T. harzianum WKY1 and its filtrate significantly reduced disease severity and improved sorghum plant growth.

Production of indoleacetic acid from trichoderma.

Zhang et al. (2013) compared cucumber growth promotion by the putative mutant Trichoderma harzianum T-E5 versus the wild-type SQR-T037 and fortified bioorganic fertilizers. They found that the putative T-E5 mutant improved IAA production and plant colonization ability, which had great potential for further application of T-E5 in crop production.

Bader et al. (2020). They characterized a set of Trichoderma strains isolated from nearly pristine horticultural soils of the Argentine pampas and evaluated their potential as growth promoters and as bio-controllers of Fusarium wilt disease in tomatoes. The result was that twelve strains reduced the growth of pathogenic fungi by more than 50%, and four exhibited the highest IAA production (between 13.38 and 21.14 µg/ml) and were able to solubilize phosphate (between 215.80 and 288.18 µg/ml of calcium phosphate). Tomato plants inoculated with these four strains increased chlorophyll content, shoot length, fresh and dry weight of shoots and roots, and reduced F. oxysporum wilt disease by 10-30%.

Chagas et al. (2016) determined the efficiency of Trichoderma spp. in promoting the growth of cowpea plants.

They concluded that Trichoderma isolates showed a more extraordinary ability to synthesize IAA and solubilize phosphate than controls.

Napitupulu et al. (2019) optimized environmental conditions for IAA production by Trichoderma harzianum strain InaCC F88. They report that supplementation with 1% L-tryptophan in the medium provides maximum IAA production. The most favorable initial pH and temperature for IAA production are 6.0 and 27°C, respectively. In the salinity test, the medium containing 1% NaCl produced the highest IAA formation. After four days of incubation, the IAA concentration reached equilibrium. Therefore, manipulating those factors could achieve optimal IAA production in liquid fermentation.

Nieto-Jacobo et al. (2017) show that indoleacetic acid (IAA) production is stress-dependent, and various external stimuli are associated with its production. Their results suggest the mechanisms and molecules involved in plant growth promotion by Trichoderma spp. They are multivariable and are affected by environmental conditions.

Trichoderma vs. Cancer.

Tang et al. (2020). They searched for selective growth inhibitors against cancer cells adapted to nutrient deprivation. Trichoderma lixii metabolites exhibited potent, selective cytotoxic activity against human pancreatic carcinoma PANC-1 cells cultured under glucose-starved conditions with IC50 values of 0.02 µM.

Cubeddu (2022) found that in cancer patients, high doses of cisplatin increase urinary and plasma levels of 5-hydroxy-indoleacetic acid (5-HIAA) but do not affect platelets or plasma-free serotonin. Changes in 5-HIAA levels parallel the onset and development of vomiting.

This research aimed to calculate the quantum-chemical interactions of indoleacetic acid and protein amino acids through computational quantum chemistry.

MATERIAL AND METHODS

The characterization of the IAA was done through the hyperchem simulator. The parameterization of this simulator is shown in tables 1 and 2.

Table 1: Parameters used for quantum computing molecular orbitals HOMO and LUMO.

Parameter	Value	Parameter	Value
Total, charge	0	Polarizability	Not
Spin Multiplicity	1	Geometry Optimization algorithm	Polak-Ribiere (Conjugate Gradient)
Spin Pairing	RHF	Termination condition RMS gradient of	0.1 Kcal/Amol
State Lowest Convergent Limit	0.01	Termination condition or	1000 maximum cycles
Interaction Limit	50	Termination condition or	In vacuo
Accelerate Convergence	Yes	Screen refresh period	1 cycle

Table 2. Parameters used for visualizing the map of the electrostatic potential of the molecules

Parameter	Value	Parameter	Value
Molecular Property	Property Electrostatic Potential	Contour Grid increment	0.05
Representation	3D Mapped Isosurface	Mapped Function Options	Default
Isosurface Grid: Grid Mesh	Coarse	Transparency level	A criteria
Size			
Isosurface Grid: Grid Layout	Default	Isosurface Rendering: Total charge density contour value	0.015
Contour Grid: Starting Value	Default	Rendering Wire Mesh	

The entire basis of the calculation was made with the theory of the electron transfer coefficient. González (2017).
The characterization of the twenty amino acids was also carried out with this simulator.

RESULTS

Figures 2-A and 2-B show the results of the geometrization and the map of the electrostatic potential of the IAA, respectively. In this case, the electrostatic potential has units of electron volts/Bohr radius (eV/a°).

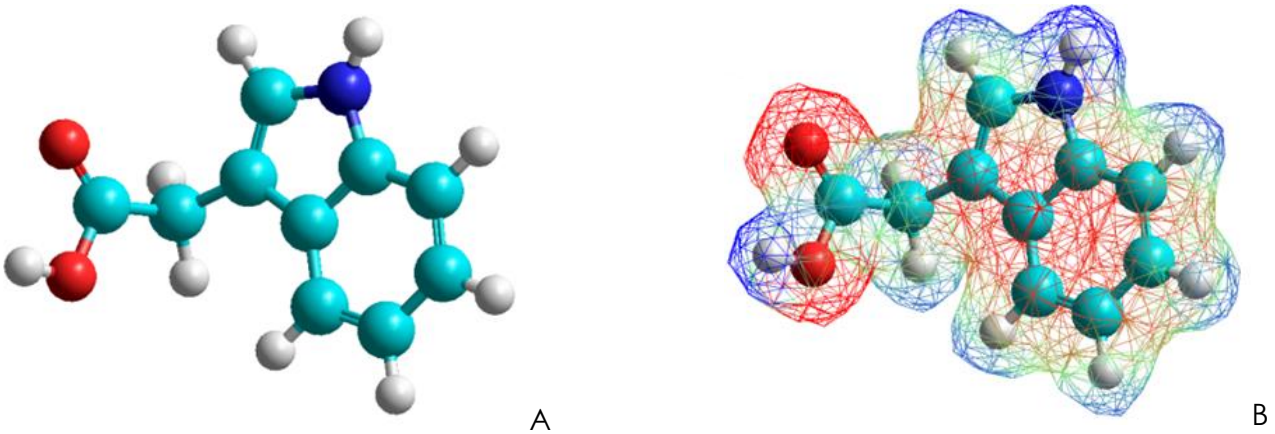

A B

Figure 2. Molecules of indoleacetic acid. A) C = cyan, N = blue, O = red, H = white. B) Electrostatic potential. Red = negative pole, blue = positive pole, green = neutral.

Figure 3 shows us the map and the calculations of the HOMO (-8.544069 eV) of the IAA. This molecular orbital is observed on the rings that form the indole.

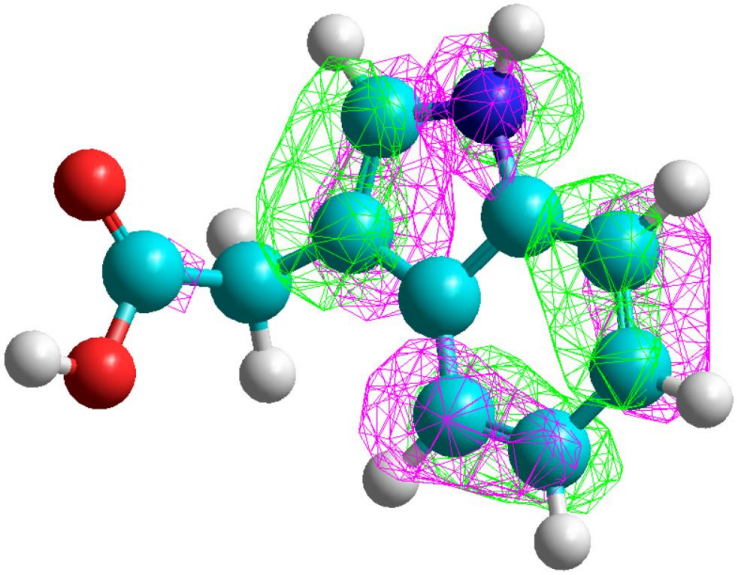

Figure 3. HOMO of the indoleacetic acid molecule.

Figure 4 shows the cloud and calculations of the LUMO (-0.06923014 eV). The cloud from this orbital is shown above the IAA rings as well.

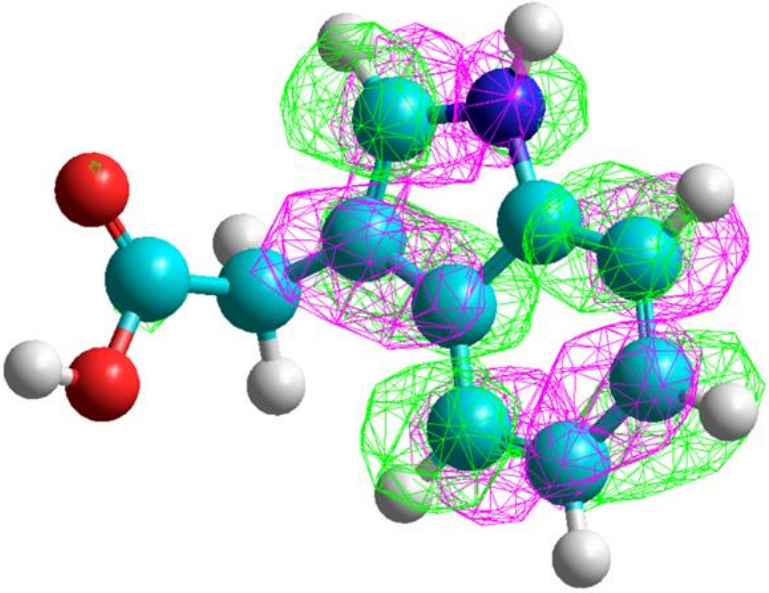

Figure 4. LUMO of the indoleacetic acid molecule.

These two orbitals are so close together that we can interpret them as "filled and not filled with electrons at the same time.". For this reason, these molecules can naturally form micelles.

Where:
Bg = Forbidden band.
EP = Electrostatic Potential.
ETC = Electron Transfer Coefficient.

The ETC is the number of times the Bohr radius (a°) that an electron needs to jump from the HOMO of one molecule to the LUMO of another molecule. Although the equivalent unit is the Bohr radius, it is sometimes customary to be dimensionless.
Another interpretation. The ETC is the number of times the electron needs the electrostatic potential to jump the band gap from one molecule A1 to another molecule A2 of the same chemical species or different chemical species, but never within the same molecule (band gap).
In table 3, the ETC of the IAA is observed in interaction 21 of the quantum well. This observation shows that IAA is the most unstable pure substance among the 20 AA. The ETC of the Arg is shown up to the bottom of the hole (interaction number 1). This interaction number 1 tells us that Arg is the most stable substance. González-Pérez (2022).

Table 3. Amino acids and IAA ordered. QUANTUM WELL.

N	Reducer	Oxidizing	HOMO	LUMO	BG	d-	d+	EP	ETC
21	IAA	IAA	-8.544	-0.069	8.475	-0.019	0.145	0.164	51.676
20	Val	Val	-9.914	0.931	10.845	-0.131	0.109	0.240	45.188
19	Ala	Ala	-9.879	0.749	10.628	-0.124	0.132	0.256	41.515
18	Leu	Leu	-9.645	0.922	10.567	-0.126	0.130	0.256	41.279
17	Phe	Phe	-9.553	0.283	9.836	-0.126	0.127	0.253	38.879
16	Gly	Gly	-9.902	0.902	10.804	-0.137	0.159	0.296	36.500
15	Ser	Ser	-10.156	0.565	10.721	-0.108	0.198	0.306	35.037
14	Cys	Cys	-9.639	-0.236	9.403	-0.129	0.140	0.269	34.956
13	Glu	Glu	-10.374	0.438	10.812	-0.111	0.201	0.312	34.655
12	Ile	Ile	-9.872	0.972	10.844	-0.128	0.188	0.316	34.316
11	Thr	Thr	-9.896	0.832	10.728	-0.123	0.191	0.314	34.167
10	Gln	Gln	-10.023	0.755	10.778	-0.124	0.192	0.316	34.108
9	Asp	Asp	-10.370	0.420	10.790	-0.118	0.204	0.322	33.509
8	Asn	Asn	-9.929	0.644	10.573	-0.125	0.193	0.318	33.249
7	Lys	Lys	-9.521	0.943	10.463	-0.127	0.195	0.322	32.495
6	Pro	Pro	-9.447	0.792	10.238	-0.128	0.191	0.319	32.095
5	Trp	Trp	-8.299	0.133	8.431	-0.112	0.155	0.267	31.577
4	Tyr	Tyr	-9.056	0.293	9.349	-0.123	0.193	0.316	29.584
3	His	His	-9.307	0.503	9.811	-0.169	0.171	0.340	28.855
2	Met	Met	-9.062	0.145	9.207	-0.134	0.192	0.326	28.243
1	Arg	Arg	-9.176	0.558	9.734	-0.165	0.199	0.364	26.742

Table 4 lists the ETCs of the oxidation-reduction interactions of IAA acid and the 20 amino acids of proteins. This table shows the location of each IAA interaction. It should be remembered that the most likely interactions with the highest affinity range from quartile 1 to quartile 4.

Table 4. ETCs of the oxidation-reduction interactions of IAA and AAs.

N	Reducer	Oxidizing	HOMO	LUMO	BG	δ–	δ+	EP	ETC
Fourth quartile									
61	IAA	Val	-8.544	0.931	9.475	-0.019	0.109	0.128	74.025
60	IAA	Leu	-8.544	0.922	9.466	-0.019	0.130	0.149	63.531
59	IAA	Ala	-8.544	0.749	9.293	-0.019	0.132	0.151	61.544
58	IAA	Phe	-8.544	0.283	8.827	-0.019	0.127	0.146	60.461
57	IAA	Gly	-8.544	0.902	9.446	-0.019	0.159	0.178	53.065
56	IAA	Cys	-8.544	-0.236	8.309	-0.019	0.140	0.159	52.255
55	IAA	IAA	-8.544	-0.069	8.475	-0.019	0.145	0.164	51.676
54	IAA	Trp	-8.544	0.133	8.677	-0.019	0.155	0.174	49.866
53	IAA	His	-8.544	0.503	9.047	-0.019	0.171	0.190	47.617
52	IAA	Ile	-8.544	0.972	9.516	-0.019	0.188	0.207	45.970
51	Val	Val	-9.914	0.931	10.845	-0.131	0.109	0.240	45.188
50	IAA	Thr	-8.544	0.832	9.376	-0.019	0.191	0.210	44.648
49	IAA	Pro	-8.544	0.792	9.336	-0.019	0.191	0.210	44.457
48	IAA	Lys	-8.544	0.943	9.487	-0.019	0.195	0.214	44.331
47	IAA	Gln	-8.544	0.755	9.299	-0.019	0.192	0.211	44.071
Third quartile									
46	IAA	Asn	-8.544	0.644	9.188	-0.019	0.193	0.212	43.341
45	IAA	Ser	-8.544	0.565	9.109	-0.019	0.198	0.217	41.976
44	IAA	Arg	-8.544	0.558	9.102	-0.019	0.199	0.218	41.752
43	IAA	Tyr	-8.544	0.293	8.837	-0.019	0.193	0.212	41.682
42	Ala	Ala	-9.879	0.749	10.628	-0.124	0.132	0.256	41.515
41	Leu	Leu	-9.645	0.922	10.567	-0.126	0.130	0.256	41.279
40	IAA	Met	-8.544	0.145	8.689	-0.019	0.192	0.211	41.181
39	IAA	Glu	-8.544	0.438	8.982	-0.019	0.201	0.220	40.829
38	Glu	IAA	-10.374	-0.069	10.305	-0.111	0.145	0.256	40.254
37	IAA	Asp	-8.544	0.420	8.964	-0.019	0.204	0.223	40.198
36	Ser	IAA	-10.156	-0.069	10.087	-0.108	0.145	0.253	39.870
35	Asp	IAA	-10.370	-0.069	10.301	-0.118	0.145	0.263	39.166
34	Phe	Phe	-9.553	0.283	9.836	-0.126	0.127	0.253	38.879
33	Gln	IAA	-10.023	-0.069	9.954	-0.124	0.145	0.269	37.003
32	Thr	IAA	-9.896	-0.069	9.827	-0.123	0.145	0.268	36.669
Second quartile									
31	Asn	IAA	-9.929	-0.069	9.860	-0.125	0.145	0.270	36.518
30	Gly	Gly	-9.902	0.902	10.804	-0.137	0.159	0.296	36.500

29	Ala	IAA	-9.879	-0.069	9.810	-0.124	0.145	0.269	36.467
28	Ile	IAA	-9.872	-0.069	9.803	-0.128	0.145	0.273	35.908
27	Val	IAA	-9.914	-0.069	9.845	-0.131	0.145	0.276	35.669
26	Leu	IAA	-9.645	-0.069	9.576	-0.126	0.145	0.271	35.336
25	Ser	Ser	-10.156	0.565	10.721	-0.108	0.198	0.306	35.037
24	Phe	IAA	-9.553	-0.069	9.484	-0.126	0.145	0.271	34.996
23	Cys	Cys	-9.639	-0.236	9.403	-0.129	0.140	0.269	34.956
22	Cys	IAA	-9.639	-0.069	9.570	-0.129	0.145	0.274	34.925
21	Gly	IAA	-9.902	-0.069	9.833	-0.137	0.145	0.282	34.869
20	Lys	IAA	-9.521	-0.069	9.451	-0.127	0.145	0.272	34.748
19	Glu	Glu	-10.374	0.438	10.812	-0.111	0.201	0.312	34.655
18	Pro	IAA	-9.447	-0.069	9.377	-0.128	0.145	0.273	34.349
17	Ile	Ile	-9.872	0.972	10.844	-0.128	0.188	0.316	34.316
First quartile									
16	Thr	Thr	-9.896	0.832	10.728	-0.123	0.191	0.314	34.167
15	Gln	Gln	-10.023	0.755	10.778	-0.124	0.192	0.316	34.108
14	Tyr	IAA	-9.056	-0.069	8.987	-0.123	0.145	0.268	33.533
13	Asp	Asp	-10.370	0.420	10.790	-0.118	0.204	0.322	33.509
12	Asn	Asn	-9.929	0.644	10.573	-0.125	0.193	0.318	33.249
11	Lys	Lys	-9.521	0.943	10.463	-0.127	0.195	0.322	32.495
10	Met	IAA	-9.062	-0.069	8.993	-0.134	0.145	0.279	32.232
9	Pro	Pro	-9.447	0.792	10.238	-0.128	0.191	0.319	32.095
8	Trp	IAA	-8.299	-0.069	8.229	-0.112	0.145	0.257	32.021
7	Trp	Trp	-8.299	0.133	8.431	-0.112	0.155	0.267	31.577
6	Tyr	Tyr	-9.056	0.293	9.349	-0.123	0.193	0.316	29.584
5	His	IAA	-9.307	-0.069	9.238	-0.169	0.145	0.314	29.421
4	Arg	IAA	-9.176	-0.069	9.107	-0.165	0.145	0.310	29.377
3	His	His	-9.307	0.503	9.811	-0.169	0.171	0.340	28.855
2	Met	Met	-9.062	0.145	9.207	-0.134	0.192	0.326	28.243
1	Arg	Arg	-9.176	0.558	9.734	-0.165	0.199	0.364	26.742

Tables 5, 6, and 7 show a chi-square test of association.

Table 5. Summary of the oxidation-reduction interactions IAA vs. AA's

Quartile	Upper limit	Reducing	Oxidizing	Sums
First	34.167	0	5	5
Second	36.518	0	10	10
Third	43.341	7	5	12
Fourth	74.025	14	1	15
	Sums	21	21	42

Table 6. Expected values of oxidation-reduction interactions.

Quartile	Upper limit	Reducing	Oxidizing	Sums
First	34.167	2.5	2.5	5

Second	36.518	5	5	10
Third	43.341	6	6	12
Fourth	74.025	7.5	7.5	15
	Sums	21	21	42

Table 7. Chi square statistics

Quartile	Upper limit	Reducing	Oxidizing	Sums
First	34.167	2.5	2.5	5
Second	36.518	5	5	10
Third	43.341	0.16666667	0.16666667	0.33333333
Fourth	74.025	5.63333333	5.63333333	11.2666667
	Sumas	13.3	13.3	**26.6**

Experimental chi square = 26.6; Theoretical chi square = 7.8147279.

The null hypothesis is rejected, and the variables are associated. The associated variables mean that the distribution of the quadrants and the oxidation-reduction interactions present a nonlinear pattern (in two dimensions).

The nonlinear pattern is a skewed normal function presented in the figure.

This figure shows the quantum anchor of the IAA in the same quantum well. It is immediately noticeable that the quantum anchor of the IAA is biased up or to the right if it swaps the "x" axis with the "y" axis; Due to the bias, the cluster of oxidation-reduction interactions is grouped at the bottom of the well.

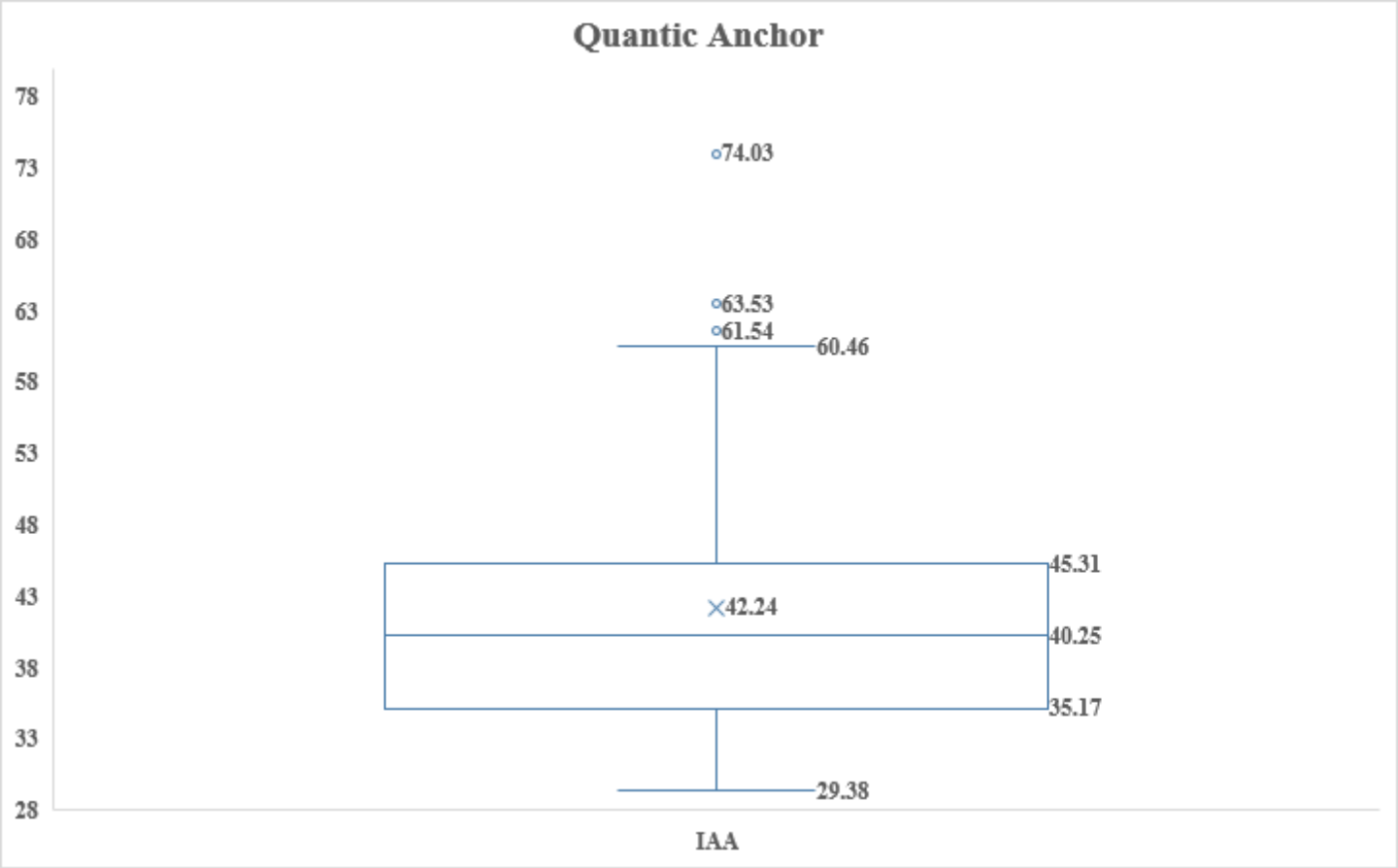

Figure 5. Box-and-whisker plot of the ETCs of quantum-chemical interactions of amino acids and indole acetic acid (quantum anchoring).

Table 8 shows the summary of this box-and-whisker statistical technique. The anchor density (last column) accumulates at the bottom of the hole. This observation demonstrates the positive bias.

Table 8. Summary of the whiskers and box plot.

Boundaries	ETC	Width	Band	Frequency	Location	Density
Higher	74.03					
Top top mustache	60.46	13.57	Superior atypical	4	9.76%	0.29
Top top bar	45.31	15.15	Top mustache	5	12.20%	0.33
Top bottom bar	40.31	5.00	Top bar	10	24.39%	2.00
Bottom bottom bar	35.17	5.14	Bottom bar	12	29.27%	2.33
Lower lower mustache	29.38	5.79	Lower mustache	10	24.39%	1.73
Lower limit	29.38	0.00	lower outlier	0	0.00%	
			Sum	41	100.00%	

Another observation is that the anchors are denser in the lower whisker and the two bars.

Only the two most robust interactions in a mixture of loose and protein-bound amino acids are presented in Table 9.

The total of the "quantum soup" interactions are 441.

Table 9. ETCs of the strongest interactions of the quantum soup.

N	Reducer	Oxidizing	HOMO	LUMO	BG	δ–	δ+	EP	ETC
441	IAA	Val	-8.544069	0.9311865	9.4752555	-0.019	0.109	0.128	74.025
Interactions suppressed due to lack of space									
48	His	IAA	-9.307456	-0.06923014	9.23822586	-0.169	0.145	0.314	29.421
47	Arg	IAA	-9.176235	-0.06923014	9.10700486	-0.165	0.145	0.31	29.377
Interactions suppressed due to lack of space									
1	Arg	Asp	-9.176235	0.4201105	9.5963455	-0.165	0.204	0.369	26.006

These two interactions are in the first quartile of the quantum well. The most probable and robust interactions are grouped in this first quartile. Therefore, Arg and His are the two AAs most closely related to IAA, even in AAs sequenced as proteins.

If we compare in a general way the oxidation-reduction table and the quantum soup, we can see that there are interactions outside and inside the whisker diagram. These interactions do not involve IAA. They are interactions that protect or preserve the structure of proteins from IAA attack or anchoring. We can predict that IAA does not destroy cancerous tumors.

CONCLUSIONS

Goal.

This research aimed to calculate the quantum-chemical interactions of indoleacetic acid and protein amino acids through computational quantum chemistry.

Thesis. We find that:

1. IAA is the most unstable substance compared to the 20 AAs.
2. The most robust IAA interactions in terms of electron affinity with AAs are Arg and His.

3. These interactions are followed by three more, making a total of 5 interactions in the first quartile.
4. IAA behaves as an oxidizing agent in all these first quartile interactions.
5. IAA interactions increase as the number of quartiles increases.
6. IAA anchorage in protein amino acids presents a nonlinear pattern.
7. The pattern presented by this anchor is "normal" with a positive bias.
8. There is a difference between the quantum soup well and the box-and-whisker plot of the nonlinear pattern.
9. This difference is some interactions where the IAA does not intervene.

Corollaries and arguments.

1. We calculate the ETCs of each substance to report the oxidation-reduction interactions and the quantum soup in tables.
2. We rely on the ETC theory already published in 2017. To do all the quantum calculations.
3. We did a chi-square hypothesis association test to determine a nonlinear pattern.
4. We made a box-and-whisker plot to demonstrate this nonlinear pattern.

In general, we can predict that cancerous tumors are not annihilated by applying IAA as the only treatment.

REFERENCES

Bader, A. N., Salerno, G. L., Covacevich, F., & Consolo, V. F. (2020). Native Trichoderma harzianum strains from Argentina produce indole-3 acetic acid and phosphorus solubilization, promote growth and control wilt disease on tomato (Solanum lycopersicum L.). Journal of King Saud University-Science, 32(1), 867-873.

Chagas, L. F. B., De Castro, H. G., Colonia, B. S. O., De Carvalho Filho, M. R., Miller, L. D. O., & Chagas, A. F. J. (2016). Efficiency of Trichoderma spp. as a growth promoter of cowpea (Vigna unguiculata) and analysis of phosphate solubilization and indole acetic acid synthesis. Brazilian Journal of Botany, 39(2), 437-445.

Cubeddu, L. X. (1992, December). Mechanisms by which cancer chemotherapeutic drugs induce emesis. In Seminars in oncology (Vol. 19, No. 6 Suppl 15, pp. 2-13).

Ebrahimi, N., Amirmahani, F., Sadeghi, B., & Ghanaatian, M. (2021). Trichoderma longibrachiatum derived metabolite as a potential source of anti-breast-cancer agent. Biologia, 76(5), 1595-1601.

González, M. (2017). Quantum Theory of the Electron Transfer Coefficient. International Journal of Advanced Engineering, Management and Science. Vol-3, Issue-10, Oct- 2017. 1024-1028.

González-Pérez, M., Vázquez-González, C., Ortiz, A., Camarillo-Rojas, CR., Castro-Díaz, AS., Gómez Flores,D., Lora-Sánchez, DC. Quantum-chemical analysis of the interactions of eugenol vs. nitrogenous bases of the nucleic acids RNA and DNA. J.Bio.Innov11(3), pp: 873-880, 2022.

Gravel, V., Antoun, H., & Tweddell, R. J. (2007). Growth stimulation and fruit yield improvement of greenhouse tomato plants by inoculation with Pseudomonas putida or Trichoderma atroviride: possible role of indole acetic acid (IAA). Soil Biology and Biochemistry, 39(8), 1968-1977.

Napitupulu, T. P., Kanti, A., & Sudiana, I. M. (2019, August). Evaluation of the environmental factors modulating indole-3-acetic acid (IAA) production by Trichoderma harzianum InaCC F88. In IOP Conference Series: Earth and Environmental Science (Vol. 308, No. 1, p. 012060). IOP Publishing.

Nieto-Jacobo, M. F., Steyaert, J. M., Salazar-Badillo, F. B., Nguyen, D. V., Rostás, M., Braithwaite, M., ... & Mendoza-Mendoza, A. (2017). Environmental growth conditions of Trichoderma spp. affect indole acetic acid derivatives, volatile organic compounds, and plant growth promotion. Frontiers in plant science, 102.

Saber, W. I., Ghoneem, K. M., Rashad, Y. M., & Al-Askar, A. A. (2017). Trichoderma harzianum WKY1: an indole acetic acid producer for growth improvement and anthracnose disease control in sorghum. Biocontrol Science and Technology, 27(5), 654-676.

Saravanakumar, K., Mandava, S., Chellia, R., Jeevithan, E., Yelamanchi, R. S. B., Mandava, D., ... & Wang, M. H. (2019). Novel metabolites from Trichoderma atroviride against human prostate cancer cells and their inhibitory effect on Helicobacter pylori and Shigella toxin producing Escherichia coli. Microbial pathogenesis, 126, 19-26.

Tang, R., Kimishima, A., Ishida, R., Setiawan, A., & Arai, M. (2020). Selective cytotoxicity of epidithiodiketopiperazine DC1149B, produced by marine-derived Trichoderma lixii on the cancer cells adapted to glucose starvation. Journal of natural medicines, 74(1), 153-158.

Zhang, F., Yuan, J., Yang, X., Cui, Y., Chen, L., Ran, W., & Shen, Q. (2013). Putative Trichoderma harzianum mutant promotes cucumber growth by enhanced production of indole acetic acid and plant colonization. Plant and Soil, 368(1), 433-444.